Article

Discrimination of Nitroxyl and Nitric Oxide by Water-Soluble Mn(III) Porphyrins

Marcelo A. Mart, Sara E. Bari, Daro A. Estrin, and Fabio Doctorovich

J. Am. Chem. Soc., **2005**, 127 (13), 4680-4684• DOI: 10.1021/ja044632n • Publication Date (Web): 11 March 2005

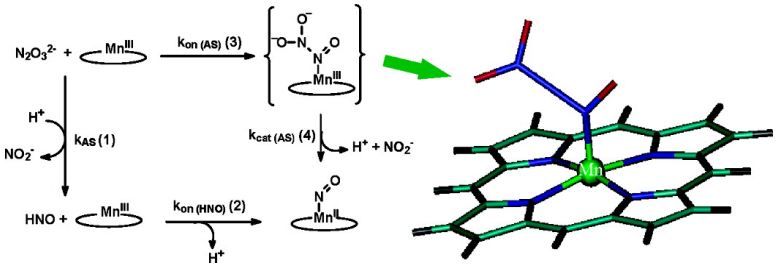

More About This Article

Additional resources and features associated with this article are available within the HTML version:

- Supporting Information
- Links to the 4 articles that cite this article, as of the time of this article download
- Access to high resolution figures
- Links to articles and content related to this article
- Copyright permission to reproduce figures and/or text from this article

View the Full Text HTML

J|A|C|S
ARTICLES
Published on Web 03/11/2005

Discrimination of Nitroxyl and Nitric Oxide by Water-Soluble Mn(III) Porphyrins

Marcelo A. Martí, Sara E. Bari, Darío A. Estrin, and Fabio Doctorovich*

Contribution from the Departamento de Química Inorgánica, Analítica y Qca. Física/ INQUIMAE-CONICET, Facultad de Ciencias Exactas y Naturales, Universidad de Buenos Aires, Ciudad Universitaria, Pab II, P. 3, Buenos Aires (C1428EHA), Argentina

Received September 3, 2004; E-mail: doctorovich@qi.fcen.uba.ar

Abstract: The water-soluble manganese(III) *meso*-tetrakis (*N*-ethylpyridinium-2-yl) porphyrin (Mn^{III}TEPyP) and manganese(III) *meso*-(tetrakis(4-sulfonato-phenyl)) porphyrinate (Mn^{III}TPPS) are able to chemically distinguish between HNO and NO donors, reacting with the former in a fast, efficient, and selective manner with concomitant formation of the $\{MnNO\}^7$ complex ($k_{on(HNO)} \approx 10^5\ M^{-1}\ s^{-1}$), while they are inert or react very slowly with NO donors. DFT calculations and kinetic data suggest that HNO trapping is operative at least in the case of Mn^{III}TPPS, while catalytic decomposition of the HNO donors (sodium trioxodinitrate and toluene sulfohydroxamic acid) seems to be the main pathway for Mn^{III}TEPyP. In the presence of oxygen, the product Mn^{II}TEPyP(NO) oxidizes back to Mn^{III}TEPyP, making it possible to process large ratios of nitroxyl donor with small amounts of porphyrin.

Introduction

Several recent studies showing distinct pharmacological effects for nitric oxide (NO) and nitroxyl (HNO/NO^-) donors are conclusive on the coexistence of both species in certain tissues.[1] Selective, efficient trapping of NO with a variety of spin-trap reagents is used as a discriminating tool, with controversial results.[2] Cysteine is currently used in HNO/NO blocking experiments, but chemical discrimination of both species requires the characterization of final products.[3,4] Unequivocal discrimination of HNO and NO still remains critical for the interpretation of the ongoing research in this field. Heme proteins[5] and isolated water-soluble ferric porphyrins[6] have been shown to react fast and efficiently with nitroxyl donors such as sodium trioxodinitrate ($Na_2N_2O_3$, Angeli's salt, AS),[7] or toluene sulfohydroxamic acid (TSHA), a derivative of Piloty's acid,[8] yielding ferrous nitrosyl compounds. However, the ferric porphyrins lead to the same reaction products as those obtained with excess NO,[9] through a reductive nitrosylation mechanism.[10] Among porphyrinic compounds, only myoglobin[11] and $[Ru(ttp)]^+$ (ttp = tetratolylporphyrinato dianion)[12] have been reported to be capable of trapping HNO.

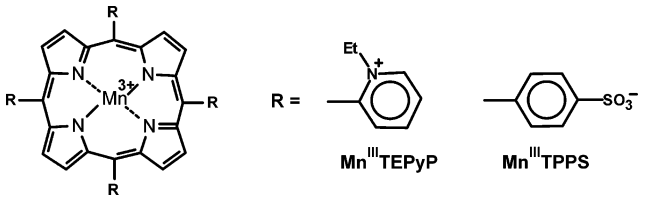

Figure 1. Structures of Mn^{III}TEPyP and Mn^{III}TPPS.

Based on the low reactivity of Mn(III) porphyrins toward NO,[13] we explored the reaction of the water-soluble manganese(III) *meso*-tetrakis (*N*-ethylpyridinium-2-yl) porphyrin (Mn^{III}TEPyP) and manganese(III) *meso*-tetrakis(4-sulfonato-phenyl) porphyrinate (Mn^{III}TPPS) (Figure 1) with the HNO

(1) (a) Pagliaro, P. *Life Sci.* **2003**, *73*, 2137−49. (b) Wink, D. A.; Miranda, K. M.; Katori, T.; Mancardi, D.; Thomas, D. D.; Ridnour, L.; Espey, M. G.; Feelisch, M.; Colton, C. A.; Fukuto, J. M.; Pagliaro, P.; Kass, D. A.; Paolocci, N. *Am. J. Physiol.: Heart Circ. Physiol.* **2003**, *285*, 2264−76. (c) Pagliaro, P.; Mancardi, D.; Rastaldo, R.; Penna, C.; Gattullo, D.; Miranda, K. M.; Feelisch, M.; Wink, D. A.; Kass, D. A.; Paolocci, N. *Free Radical Biol. Med.* **2003**, *34*, 33−43. (d) Miranda, K. M.; Paolocci, N.; Katori, T.; Thomas, D. D.; Ford, E.; Bartberger, M. D.; Espey, M. G.; Kass, D. A.; Feelisch, M.; Fukuto, J. M.; Wink, D. A. *Proc. Natl. Acad. Sci. U.S.A.* **2003**, *100*, 9196−201. (e) Paolocci, N.; Katori, T.; Champion, H. C.; St John, M. E.; Miranda, K. M.; Fukuto, J. M.; Wink, D. A.; Kass, D. A. *Proc. Natl. Acad. Sci. U.S.A.* **2003**, *100*, 5537−42. (f) Paolocci, N.; Saavedra, W. F.; Miranda, K. M.; Martignani, C.; Isoda, T.; Hare, J. M.; Espey, M. G.; Fukuto, J. M.; Feelisch, M.; Wink, D. A.; Kass, D. A. *Proc. Natl. Acad. Sci. U.S.A.* **2001**, *98*, 10463−8.
(2) (a) Komarov, A. M.; Reif, A.; Schmidt, H. H. *Methods Enzymol.* **2002**, *359*, 18−27. (b) Xia, Y.; Cardounel, A. J.; Vanin, A. F.; Zweier, J. L. *Free Radical Biol. Med.* **2000**, *29*, 793−7. (c) Vanin, A. F.; Liu, X.; Samouilov, A.; Stukan, R. A.; Zweier, J. L. *Biochim. Biophys. Acta* **2000**, *1474*, 365−77.
(3) Pino, R. Z.; Feelisch, M. *Biochem. Biophys. Res. Commun.* **1994**, *201*, 54−62.
(4) Shoeman, D. W.; Shirota, F. N.; DeMaster, E. G.; Nagasawa, H. T. *Alcohol* **2000**, *20*, 55−9.
(5) (a) Bazylinsky, D. A.; Hollocher, T. C. *J. Am. Chem. Soc.* **1985**, *107*, 7982−6. (b) Bazylinsky, D. A.; Goretski, J.; Hollocher, T. C. *J. Am. Chem. Soc.* **1985**, *107*, 7986−91. (c) Doyle, M. P.; Mahapatro, S. N.; Broene, R. D.; Guy, J. K. *J. Am. Chem. Soc.* **1988**, *110*, 593−9. (d) Miranda, K. M.; Nims, R. W.; Thomas, D. D.; Espey, M. G.; Citrin, D.; Bartberger, M. D.; Paolocci, N.; Fukuto, J. M.; Feelisch, M.; Wink, D. A. *J. Inorg. Biochem.* **2003**, *93*, 52−60.
(6) Bari, S. E.; Marti, M. A.; Amorebieta, V. T.; Estrin, D. A.; Doctorovich, F. *J. Am. Chem. Soc.* **2003**, *125*, 15272−15273.
(7) (a) Bazylinsky, D. A.; Hollocher, T. C. *Inorg. Chem.* **1985**, *24*, 4285−4288. (b) Dutton, A. S.; Fukuto, J. M.; Houk, K. N. *J. Am. Chem. Soc.* **2004**, *126*, 3795−3800.
(8) Bonner, F. T.; Ko, Y. *Inorg. Chem.* **1992**, *31*, 2514−2519.
(9) Laverman, L. E.; Ford, P. C. *J. Am. Chem. Soc.* **2001**, *123*, 11614−11622.
(10) (a) Wayland, B. B.; Olson, L. W. *J. Am. Chem. Soc.* **1974**, *96*, 6037−6041. (b) Scheidt, W. R.; Ellison, M. K. *Acc. Chem. Res.* **1999**, *32*, 350−359. (c) Ford, P. C.; Lorkovic, I. M. *Chem. Rev.* **2002**, *102*, 993−1018.
(11) Sulc, F.; Immoos, C. E.; Pervitsky, D.; Farmer, P. *J. Am. Chem. Soc.* **2004**, *126*, 1096−1101.
(12) Lee, J.; Richter Addo, G. B. *J. Inorg. Biochem.* **2004**, *98*, 1247−1250.

10.1021/ja044632n CCC: $30.25

donors AS and TSHA, aiming at the chemical differentiation of these redox partners.

Materials and Methods

$Mn^{III}TEPyP$ and $Mn^{III}TPPS$ were purchased from Frontier Scientific. AS and TSHA were synthesized according to published literature.[14] NO-donors (sodium nitroprusside and S-nitroso-*N*-acetylpenicillamine) were purchased from Sigma-Aldrich Argentina.

Reactions of $Mn^{III}TEPyP$ and $Mn^{III}TPPS$ with AS and TSHA. All experiments were done at 25 °C in 0.1 M phosphate buffer, containing EDTA 10^{-4} M. Porphyrin concentration was 5.5×10^{-6} M, unless stated otherwise. UV−vis spectra were recorded with a HP 8453 spectrometer in a septum sealed 1 cm path quartz cuvette. All reactions were carried out under Ar atmosphere unless stated otherwise. AS and TSHA solutions were freshly prepared for each set of measurements and kept on ice. The HNO source concentration was checked before each measurement. TSHA was dissolved in ethanol 96% and added to the porphyrin solutions to a final ethanol/water ratio of less than 1%. The reaction rate was measured by following the absorbances at 454 nm ($Mn^{III}TEPyP$), 468 nm ($Mn^{III}TPPS$), 422 nm ($Mn^{II}TEPyP(NO)$), and 424 nm ($Mn^{II}TPPS(NO)$). All reactions were followed until no more spectroscopic changes were observed unless stated otherwise. Reaction times ranged from 60 s to 2 h. The initial observed reaction rate for each measurement was obtained by plotting the reactant and product concentration versus time and calculating the initial rates by fitting the corresponding function. In all cases, the rate constants obtained did not differ significantly considering either reactant consumption or product formation.

Determination of the Rate Constants. The slopes and the corresponding k_{obs} for the bimolecular reactions were determined by standard fitting procedures from the initial rates versus initial donor concentration plots (Figures 3, S1, S2, and S3). Assuming that binding of trioxodinitrate to the metalloporphyrin was the rate-limiting step, the k_{obs} obtained from the plot equals the k_{on} for AS or TSHA binding.

In the cases where donor decomposition was the rate-limiting step, the following kinetic analysis was used:

$$\text{donor (TSHA or AS)} \underset{k_{-1}}{\overset{k_1}{\rightleftharpoons}} \text{HNO} \qquad (1)$$

$$\text{HNO} + Mn^{III}TPPS \xrightarrow{k_2} Mn^{II}TPPS{-}NO \qquad (2)$$

$$\text{HNO} + \text{HNO} \xrightarrow{k_3} N_2O + H_2O \qquad (3)$$

where reaction 1 represents reversible donor decomposition, reaction 2 represents HNO binding to the metalloporphyrin, and reaction 3 represents HNO dimerization. When reaction 1 is rate limiting, and applying the steady-state approximation for [HNO], all of the HNO produced through reaction 1 must be consumed in reactions 2 and 3; therefore, $V_1 = V_2 + V_3$. The donor decomposition rate V_1 and the dimerization rate constant k_3 ($k_3 = 8 \times 10^6$ M^{-1} s^{-1})[15] were known data for each measurement. Therefore, by measuring V_2 as the initial product formation rate, V_3 and accordingly [HNO] could be estimated. The back reaction of reaction 1 was not considered because its rate is negligible in comparison with reactions 2 and 3.[16] Taking the estimated [HNO] values from the initial rates (V_2) versus [HNO] plots, an estimate for $k_{on(HNO)}$ can be obtained from the slope (Figures 6 and 7). The error estimates in the values obtained for the rate constants were the propagated statistical error from the linear fitting that includes the standard deviation for each point.

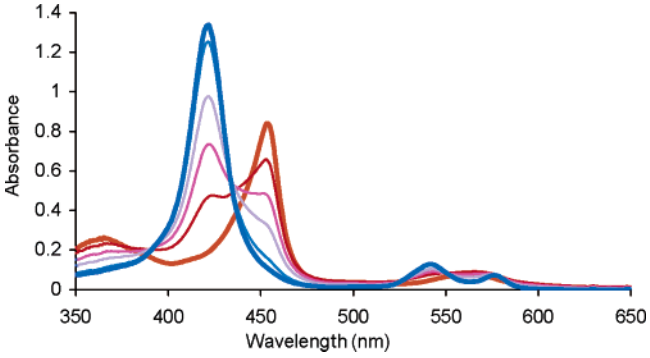

Figure 2. Spectral changes for the anaerobic reaction of $Mn^{III}TEPyP$ (5×10^{-6} M, $\lambda_{max} = 455$ nm) with AS (5×10^{-6} M), at 25 °C in 0.1 M phosphate buffer, containing EDTA 10^{-4} M. $Mn^{III}TEPyP$, red line; $Mn^{II}TEPyP(NO)$, blue line ($\lambda_{max} = 422$ nm).

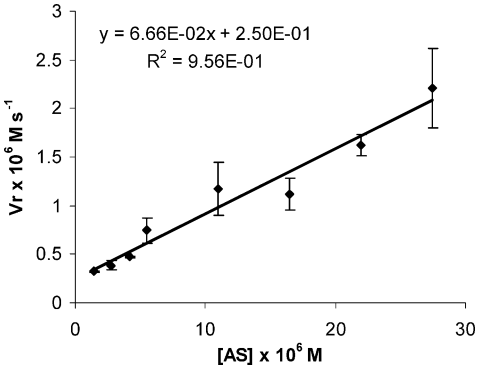

Figure 3. Initial observed reaction rates versus initial AS concentration at pH 7 (phosphate buffer, 25 °C), for the reaction of $Mn^{III}TEPyP$ with AS. $[Mn^{III}TEPyP] = 5.5 \times 10^{-6}$ M. Values are the mean ± standard deviation of at least three independent measurements.

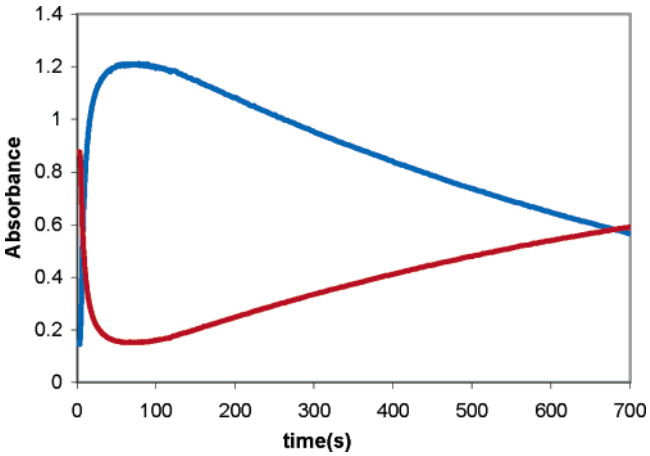

Figure 4. Reaction of AS with $Mn^{III}TEPyP$ under air atmosphere ($Mn^{II}TEPyP$, red line, $\lambda_{max} = 454$ nm; $Mn^{II}TEPyP{-}NO$, blue line, $\lambda_{max} = 422$ nm).

Computational Methods. All computations were performed at the DFT level with the SIESTA code.[17] The SIESTA method has shown

(13) Spasojevic, I.; Batinic-Haberle, I.; Fridovich, I. *Nitric Oxide Biol. Chem.* **2000**, *4*, 526−533.
(14) Hughes, M. N.; Cammack, R. *Methods Enzymol.* **1999**, *301*, 279−81.
(15) Shafirovich, V.; Lymar, V. S. *Proc. Natl. Acad. Sci. U.S.A.* **2002**, *99*, 7340−7345.
(16) (a) Akhtar, M. J.; Lutz, C. A.; Bonner, F. T. *Inorg. Chem.* **1979**, *18*, 2369. (b) Hughes, M. N.; Wimbledon, P. E. *J. Chem. Soc., Dalton Trans.* **1976**, *8*, 703−7.
(17) (a) Soler, J. M.; Artacho, E.; Gale, J.; García, A.; Junquera, J.; Ordejón, P.; Sánchez-Portal, D. *J. Phys.: Condens. Matter* **2002**, *14*, 2745. (b) Scherlis, D. A.; Martí, M. A.; Ordejón, P.; Estrin, D. A. *Int. J. Quantum Chem.* **2002**, *90*, 1505−1514. (c) Martí, M. A.; Crespo, A.; Bari, S. E.; Doctorovich, F. A.; Estrin, D. A. *J. Phys. Chem. B* **2004**, *108*, 18073−18080.

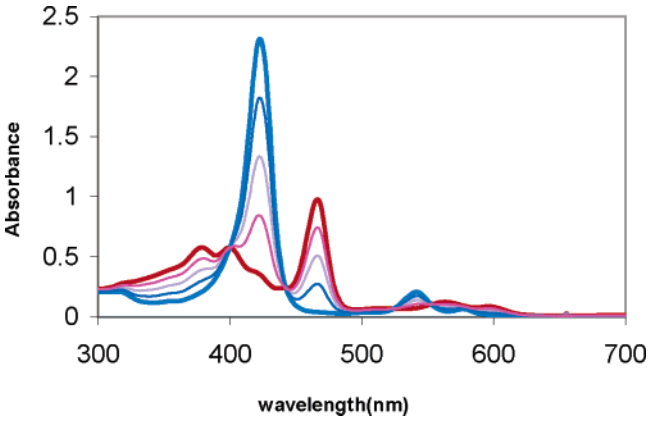

Figure 5. Spectral changes for the anaerobic reaction of $Mn^{III}TPPS$ (5×10^{-6} M, $\lambda_{max} = 468$ nm) with AS (5×10^{-6} M), at 25 °C in 0.1 M phosphate buffer, containing EDTA 10^{-4} M. $Mn^{III}TPPS$, red line; $Mn^{II}TPPS(NO)$, blue line ($\lambda_{max} = 424$ nm).

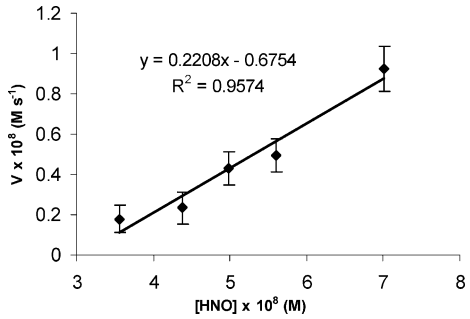

Figure 6. Initial observed reaction rates versus estimated [HNO] at pH 7 (0.1 M phosphate buffer, 25 °C), for the reaction of $Mn^{III}TPPS$ (5×10^{-6} M) with AS. Values are the mean ± standard deviation of at least three independent measurements.

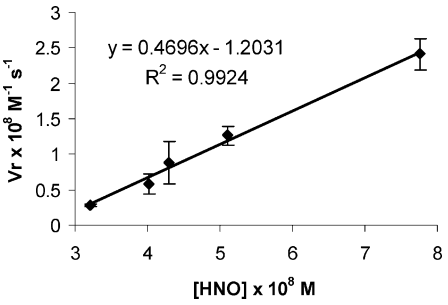

Figure 7. Initial observed reaction rates versus estimated [HNO] at pH 10 (phosphate buffer, 25 °C), for the reaction of $Mn^{III}TPPS$ (5×10^{-6} M) with TSHA. Values are the mean ± standard deviation of at least three independent measurements.

an excellent performance for medium and large systems and has also proved to be appropriate for biomolecules and, specifically, for heme models.[18] The use of standard norm-conserving pseudopotentials[19] avoids the computation of core electrons, smoothing at the same time the valence charge density. In our study, the nonlinear partial-core correction was applied to the iron atom.[20] Basis functions consist of localized (numerical) pseudoatomic orbitals, projected on a real space grid to compute the Hartree potential and exchange correlation potentials matrix elements. For all atoms, basis sets of double ξ plus polarization quality were employed, with a pseudoatomic orbital energy shift of 25 meV and a grid cutoff of 150 Ry. Calculations were performed using the generalized gradient approximation functional proposed by Perdew, Burke, and Ernzerhof.[21] This combination of functional, basis sets, and grid parameters has been already validated for heme models.[18] The model used consisted of a porphyrin saturated with hydrogen atoms in all side chains plus the corresponding ligand (NO or AS). The final system consisted of about 40 atoms.

Scheme 1

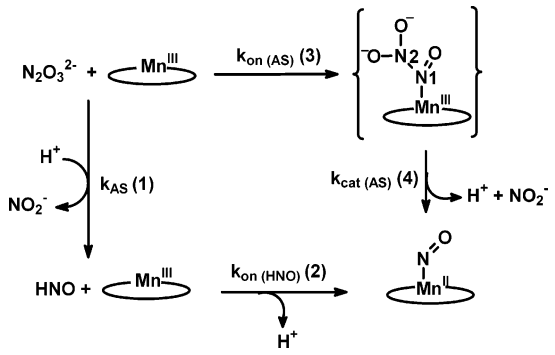

Results and Discussion

Reaction of $Mn^{III}TEPyP$ with AS in Anaerobic Solutions. When aqueous solutions of AS were added to $Mn^{III}TEPyP$ solutions under inert atmosphere in equimolar ratios, total conversion of $Mn^{III}TEPyP$ to $Mn^{II}TEPyP(NO)$ was observed in less than 1 min (Figure 2). The reaction product was identified by comparison with the one obtained from the same starting material and NO in the presence of a reducing agent.[13]

No spectral changes were observed for more than 30 min when aqueous solutions of NO donors such as sodium nitroprusside or S-nitroso-*N*-acetylpenicillamine were added to $Mn^{III}TEPyP$ solutions under inert atmosphere in equimolar or excess NO donor ratios under our reaction conditions. Conversion of $Mn^{III}TEPyP$ to $Mn^{II}TEPyP(NO)$ was quantitatively observed only when a reducing agent (e.g., ascorbic acid or sodium dithionite) was added in slight excess, prior or after the addition of the NO donor. This result is consistent with that obtained by Spajosevic et al.,[13] who showed that reductive nitrosylation was very slow for this cationic Mn(III) porphyrin ($t_{1/2} \approx 60$ min with excess NO(g)).

Kinetic Analysis. Figure 2 shows the shift of the Soret band of $Mn^{III}TEPyP$ after the addition of AS; the 33 nm blue-shift allowed direct measurement of the initial reaction rates for different molar ratios. The initial rate value obtained was independent of the set of spectroscopic measures (reactant or product) considered. A proposed mechanism for the reaction of Mn porphyrins with AS is shown in Scheme 1, where k_{AS} is AS decomposition rate constant, $k_{cat(AS)}$ is AS decomposition rate constant catalyzed by the porphyrin, and $k_{on(AS)}$ and $k_{on(HNO)}$ are AS and HNO coordination rate constants, respectively. The back reactions were considered negligible under our reaction conditions.

In all of the experiments, only $Mn^{III}TEPyP$ and $Mn^{II}TEPyP(NO)$ were detected by UV−vis spectroscopy, suggesting that the hypothetical complex $Mn^{III}TEPyP(AS)$, if formed, is in a small steady-state concentration. If product formation occurs through reactions 1 and 2, then AS decomposition (k_{AS}) must be rate limiting. At pH 7, AS decomposes with a half-life of 866 s.[7,16] Under the same reaction conditions, however, the equimolar reaction had a half-life of only 5 s, indicating that

(18) Martí, M. A.; Scherlis, D. A.; Doctorovich, F.; Ordejon, P.; Estrin, D. A. *J. Biol. Inorg. Chem.* **2003**, *6*, 595−600.
(19) Troullier, N.; Martins, J. L. *Phys. Rev. B* **1991**, *43*, 1993.
(20) Louie, S. G.; Froyen, S.; Cohen, M. L. *Phys. Rev. B* **1982**, *26*, 1738.
(21) Perdew, J. P.; Burke, K.; Ernzerhof, M. *Phys. Rev. Lett.* **1996**, *77*, 3865.

the decomposition rate was 173 times faster in the presence of the metalloporphyrin. These results suggest that AS decomposition is not rate limiting. In this scenario, the product is probably formed through reactions 3 and 4 (Scheme 1), and AS coordination is the expected rate-limiting step, with N−N cleavage promoted by the metalloporphyrin. From the initial reaction rate versus [AS] plot (Figure 3), $k_{on(AS)}$ was calculated as mentioned in Materials and Methods.

To further confirm the catalytic effect of the porphyrin on AS decomposition, the reaction was performed in phosphate buffer at pH 10, where the donor is mainly in its dianionic, stable form ($N_2O_3^{2-}$, $t_{1/2} = 120$ min, p$K_{a2} = 9.7$).[7,15,16,22] As in the pH 7 case, the equimolar reaction has a half-life of only 3−5 s, indicating that reaction 3 is the rate-limiting step (Scheme 1). The reaction rate was first order in [AS], for AS/porphyrin ratios from 0.2 to 2:1. For higher [AS]/[Mn^{III}TEPyP] ratios, the reaction rate becomes almost independent of [AS], and step 4 seems to become rate limiting. The first-order rate constant $k_{cat(AS)}$ for Mn^{III}TEPyP at AS saturating concentrations is 5×10^{-1} s^{-1} (Figure S1), about 1000 times larger than that for the uncatalyzed reaction.

DFT Calculations. To obtain additional insight on the possible existence of the intermediate complex between Mn^{III}TEPyP and AS, DFT calculations with the SIESTA code were performed.[17] All calculations used a simplified Mn(III) porphyne (Mn^{III}P) in vacuo, as the model system. The calculations showed that the hypothetical complex depicted in Scheme 1 is a minimum in the potential energy surface, 16 kcal/mol more stable than the complexes with AS bound to the metal center through any of the oxygen atoms. The results also showed that the N1−N2(AS) bond length is significantly larger in the Mn^{III}P(AS) complex than in free AS (2.62 vs 1.37 Å). (N1 is the nitrogen atom bonded to the O that gives rise to HNO, N2 is the nitrogen atom that yields nitrite; see Scheme 1 and Figure S6.) Furthermore, N1−N2(AS) bond dissociation energy in free AS (44.3 kcal/mol) doubles that of the Mn^{III}P(AS) complex (19.5 kcal/mol). These data support the catalytic AS decomposition role of the porphyrin, mediated by AS coordination.

Reaction of Mn^{III}TEPyP with AS in Aerated Solutions. Mn^{III}TEPyP forms the Mn(II) nitrosyl derivative upon reaction with AS in the presence of O_2, with almost stoichiometric yield and with the same reaction rate as that observed under argon atmosphere (Figure S4). However, O_2 promotes decomposition of Mn^{II}TEPyP(NO), with a $t_{1/2}$ of a few minutes, yielding Mn^{III}TEPyP (Figure 4). Several cycles of Mn^{II}TEPyP(NO) formation and reoxidation can be achieved by adding AS after decomposition of Mn^{II}TEPyP(NO) (Figure S5).

Reaction of Mn^{III}TEPyP with TSHA in Anaerobic Solutions. When solutions of TSHA were added to degassed Mn^{III}TEPyP, Mn^{II}TEPyP(NO) was obtained, as shown by the UV/vis spectra. At pH 7, TSHA is mainly in the RNHOH form and decomposes slowly ($k_{TSHA,\ pH\ 7} \leq 5 \times 10^{-5}$ M^{-1} s^{-1}, $t_{1/2} = 230$ min).[8] At pH 10, deprotonation leads to two predominant species in equilibrium (R−N−OH ⇆ R−NH−O^-), promoting spontaneous decomposition ($k_{TSHA,\ pH\ 10} = 3.5 \times 10^{-4}$ M^{-1} s^{-1}, $t_{1/2} = 33$ min).[8] Under stoichiometric reaction conditions, a $t_{1/2} =$ 3−5 s was found at pH 10. As in the AS case, the accelerated observed decomposition rate of TSHA points to a mechanism in which TSHA interacts directly with the metalloporphyrin, which then catalyzes its decomposition. From the plot of the initial reaction rate versus TSHA concentration, the rate constant is obtained for TSHA binding to the metalloporphyrin.

At pH 7 the picture is more complex because the observed half-life for the equimolar reaction is $t_{1/2} = 33$ min as compared to the $t_{1/2} = 230$ min for spontaneous decomposition. The small rate increase observed at pH 7 could be due to the reversibility of TSHA decomposition:[8] HNO trapping by Mn^{III}TEPyP diminishes the back reaction, more important in this case than for AS, increasing the observed donor decomposition rate. However, a catalytic effect as in the pH 10 case cannot be ruled out. Kinetic analysis of this reaction showed that HNO dimerization was negligible, because Mn^{II}TEPyP(NO) formation correlates with the amount of decomposed donor.

Reaction of Mn^{III}TPPS with AS. Although the reaction between AS and Mn^{III}TPPS (an anionic metalloporphyrin) at pH 7 shows spectral changes similar to those of the reaction with Mn^{III}TEPyP, a large excess of AS was required to drive this reaction to completion. Spectral changes for the starting metalloporphyrin and the Mn^{II}(NO) product are shown in Figure 5.

Kinetic Analysis. For an equimolar ratio between AS and Mn^{III}TPPS, at pH 7 the reaction half-life is about 117 min. Under the same reaction conditions, AS has a half-life of 14.5 min.[7] Given the slow reaction rate (slower than AS decomposition) and the excess of AS needed to complete the reaction, it is reasonable to assume that AS decomposition is the rate-limiting step and the reaction proceeds through reactions 1 and 2 in Scheme 1. As mentioned in Materials and Methods, knowing the donor (AS) decomposition rate and the dimerization rate constant, [HNO] can be estimated by measuring the rate of Mn^{II}TPPS(NO) formation. From the corresponding plot (Figure 6) of initial reaction rate versus estimated [HNO], an approximate value of $k_{on(HNO)}$ can be obtained.

To further confirm that the catalytic effect of this anionic porphyrin on AS decomposition is negligible, we performed the reaction between AS and Mn^{III}TPPS at pH 10, where AS is stable ($t_{1/2} = 230$ min). As expected, for a 2:1 TSHA:Mn^{III}TPPS ratio, less than 2% Mn^{II}TPPS(NO) was observed after 2 h.

Reaction of Mn^{III}TPPS with TSHA. The reaction between TSHA and Mn^{III}TPPS at pH 10 shows the same spectral changes as the reaction with AS, and also excess TSHA is required to obtain 100% product yield.

Kinetic Analysis. For an equimolar ratio between TSHA and Mn^{III}TPPS, the reaction half-life is about 115 min. Under the same reaction conditions, TSHA has a half-life of a few minutes. The results are equivalent to those obtained for AS at pH 7; therefore, the same analysis is valid. From the plot of initial reaction rates versus the estimated [HNO], an approximate value of $k_{on(HNO)}$ is obtained (Figure 7). As expected, the value is close to that obtained for the reaction with AS (Table 1).

Again, to further confirm that there is a negligible catalytic effect of the negative porphyrin on TSHA decomposition, we performed the reaction between TSHA and Mn^{III}TPPS at pH 7, where TSHA is stable ($t_{1/2} = 120$ min). As expected, for a 2:1 AS:Mn^{III}TPPS ratio, less than 5% of Mn^{II}TPPS(NO) was observed after 2 h. It should be noted that, under the same reaction conditions, quantitative conversion to the Mn^{II}NO

(22) Sturrock, P. E.; Ray, J. D.; McDowell, J.; Hunt, H. R. *Inorg. Chem.* **1963**, *2*, 649.

Table 1. Nitroxyl Donors Binding Rate Constants and Nitroxyl Trapping Rate Constants

porphyrin	pH	donor	$k_{on(DONOR)}$ (M^{-1} s^{-1})	$k_{on(HNO)}$ (M^{-1} s^{-1})
Mn^{III}TEPyP	7	AS	$(1.2 \pm 0.1) \times 10^4$	
Mn^{III}TEPyP	10	AS	$(3.6 \pm 0.4) \times 10^4$	
Mn^{III}TEPyP	7	TSHA	$(8.1 \pm 0.3) \times 10^1$	
Mn^{III}TEPyP	10	TSHA	$(1.0 \pm 0.05) \times 10^4$	
Mn^{III}TPPS	7	AS		$\sim 4 \times 10^4$
Mn^{III}TPPS	10	TSHA		$\sim 9 \times 10^4$
Fe^{III}TPPS[6]	7	AS	0.5	$> 2.5 \times 10^7$

product was observed in less than 10 s in the case of Mn^{III}TEPyP. These data support the absence of a catalytic effect of Mn^{III}TPPS upon AS decomposition.

Conclusions

The cationic periphery in the acceptor metalloporphyrin Mn^{III}TEPyP is relevant in terms of reactivity toward anionic nitroxyl donors (AS or TSHA at pH 10). Anionic porphyrins such as Mn^{III}TPPS and Fe^{III}TPPS[6] show negligible catalytic activity toward the decomposition of the same donors. The fast reaction rates obtained for AS at pH 7 and pH 10, together with the DFT calculations, suggest the formation of a complex between AS and Mn^{III}TEPyP catalyzing the donor decomposition and yielding Mn^{II}TEPyP(NO) and nitrite. The charge effect plays an important role in the acceleration of TSHA decomposition rate at pH 10.

When the anionic Mn^{III}TPPS is used instead of the cationic Mn^{III}TEPyP as a trapping agent, slower reaction rates and lower product yields are obtained. With both nitroxyl sources, trapping rates are slower than the spontaneous decomposition rate, indicating that nitroxyl generation is the rate-limiting step. Kinetic analysis based on the decomposition rates of the nitroxyl donors and the rate constant values for HNO dimerization yielded the rate constant for HNO binding $k_{on(HNO)} = 4 \times 10^4$ M^{-1} s^{-1} when using AS, and $k_{on(HNO)} = 9 \times 10^4$ M^{-1} s^{-1} for TSHA. As expected, both values are very similar because the HNO binding rate constant should be independent of its chemical source. Our group[6] previously reported a value of 1×10^7 M^{-1} s^{-1} for the HNO binding rate constant to Fe^{III}TPPS ($k_{on(HNO)}$). It should be noted that this value was calculated assuming that HNO dimerization was about 100 times faster than the corresponding value used in this work. Using the lower estimate value for HNO dimerization would yield $k_{on(HNO)}$ (Fe^{III}TPPS) $\approx 1 \times 10^6$ M^{-1} s^{-1}, which is around 10 times larger than the rate constant for HNO binding to Mn^{III}TPPS obtained in this work (Table 1). Furthermore, NO binding rate constants to Fe(II) porphyrins are about 1×10^9 M^{-1} s^{-1},[9] whereas NO binding rates to Mn(II) porphyrins are lower, between 1×10^6 and 3.3×10^7 M^{-1} s^{-1}.[13]

The anionic character of the periphery of Mn^{III}TPPS does not favor the coordination of the nitroxyl donor species, and therefore catalytic decomposition of the donors is not observed.

Our experiments demonstrate that Mn(III) porphyrins are able to chemically distinguish between HNO and NO: while a fast and efficient reaction with HNO or its donors takes place, NO and its donors do not react or react very slowly, unless a strong reducing agent is added to the reaction medium. The significant shift in the Soret band upon reaction provides a potential tool for HNO quantitation in anaerobic systems. In the presence of oxygen, ineludible in most biological experiments, Mn^{II}TEPyP-(NO) oxidizes back to Mn^{III}TEPyP, making it possible to trap large ratios of nitroxyl with small amounts of porphyrin.

Acknowledgment. We thank the ANPCyT, CONICET, Fundación Antorchas, and UBA for financial support.

Supporting Information Available: Peak positions and relative absorptivities of reactants and products. Plots of V_r versus HNO source concentration. Computational details and data. This material is available free of charge via the Internet at http://pubs.acs.org.

JA044632N